Fate and Stability of Cr Following Reduction by Microbially Generated Fe(II)

Colleen M. Hansel[1], Bruce W. Wielinga[2], Scott Fendorf[1]

[1]Dept. of Geological and Environmental Sciences, Stanford University
[2]MFG, Inc., Fort Collins, CO 80525

A suite of industrial activities has lead to widespread Cr contamination within soils and natural waters. Although Cr is an essential element for humans, the hexavalent form is toxic, mutagenic, and carcinogenic (National Research Council, 1974). As such, the widespread presence of Cr in the environment poses a serious threat to human and animal welfare. The toxicity of Cr, however, is a function of oxidation state. Hexavalent Cr, which typically exists as the oxyanion chromate (CrO_4^{2-}), has a high solubility in soils and groundwater and, as a consequence, tends to be mobile in the environment. In contrast, the reduced form of chromium, Cr(III), has a limited hydroxide solubility and forms strong complexes with soil minerals (Sass and Rai, 1987). While trivalent Cr is relatively innocuous and immobile, hexavalent Cr is actively transported into cells by the sulfate transport system where it is capable of causing damage to DNA as well as indirectly generating oxygen radicals. Accordingly, reduction of Cr(VI) to Cr(III) is an important means by which the deleterious effects of this toxin are mitigated. This general process forms the fundamental basis of a large number of technologies currently being tested for remediation of chromium-contaminated soils.

Within anaerobic soils, Fe(II) and sulfide (S^{2-}) control the redox status of chromium (Fendorf *et al.*, 2000) via reactions in which the former are oxidized to Fe(III) and sulfate (SO_4^-) upon chromium reduction. Microbial activity has an indirect but crucial bearing on Cr(VI) cycling because the generation of Fe(II) and sulfide is reliant upon microbial respiration of Fe(III) and sulfate (Figure 1). Reduction and subsequent immobilization of chromate may therefore result from a coupled biotic-abiotic reaction pathway in which Fe(II)$_{(aq)}$ or H_2S produced during microbial respiration catalyzes the reduction of Cr(VI).
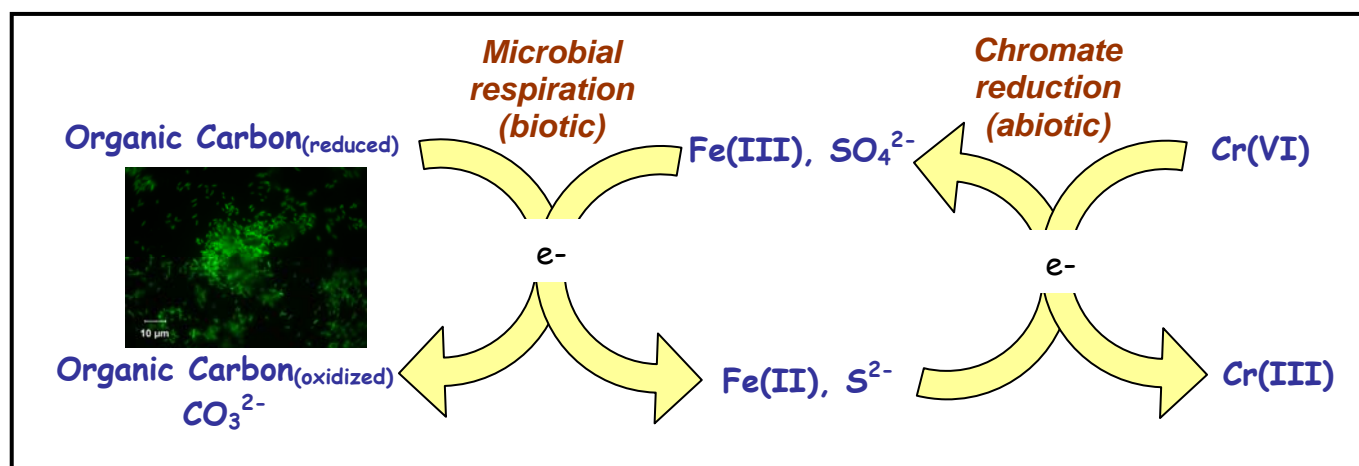

Figure 1. Oxidation/reduction cycling of Fe and sulfur is driven by microbial respiration, and can lead to chromate reduction.

The ultimate pathway of Cr(VI) reduction is of considerable pragmatic importance because it dictates the reactivity of reduced Cr(III) in the environment. In general, the solubility of Cr(III) will be controlled by the products of chromium reduction, *e.g.*, solid phases, adsorbed molecular species, or aqueous complexes, which necessitates the evaluation of reaction products. Enzymatic reduction of chromate may result in soluble Cr(III) organic complexes that can be stable for extended periods of time (James and Bartlett, 1983), while, in contrast, reduction by Fe(II) and S^{2-} results in insoluble $Cr_{1-x}Fe_x(OH)_3 \cdot nH_2O$ precipitates (Sass and Rai, 1987). The solubility of the Cr(III)-hydroxide precipitates is proportional to the ratio of Cr(III) to Fe(III), with increased quantities of Fe(III) stabilizing the solid (Sass and Rai, 1987). Understanding the composition and reactivity of these solid phases is crucial to any remediation strategy.

We have used a combination of aqueous chemical measurements and X-ray absorption spectroscopy (XAS) to elucidate the fate of Cr within flow-through reactors containing ferrihydrite ($Fe(III)(OH)_3$), a common iron-reducing bacterium (*Shewanella alga* strain BrY), and chromate (Wielinga *et al.*, 2001). In flow-cell studies, Cr(VI) was not detected in the solid-phase nor effluent at any time during reaction, indicating it was completely reduced to Cr(III). Bacterial (either enzymatic or non-enzymatic) chromate reduction was not observed; however, introduction of Cr(VI) to the flow-cells coincided with a sharp decrease in soluble Fe(II) concentrations. It can therefore be concluded that Cr(VI) was reduced by microbially generated Fe(II). The ferrous iron generated during dissimilatory Fe(III) reduction of ferric (hydr)oxides by *S. alga* had a maximum sustainable Cr(VI) reduction rate of 5.5 μg $Cr^{VI} \cdot mg\text{-}cell^{-1} \cdot h^{-1}$ (Figure 2). If the only reactant available to chromate was the initial supply of Fe(III) (as ferrihydrite) then reduction could be maintained for only ca. 70 h. For Fe(III) reduction to continue beyond 70 h, Fe within the system must be (re)cycled back to the ferric state—a redox cycle between the bacteria and chromate must be established. As shown in Figure 2, Cr(VI) reduction continued until the end of the experiment, at 168 hrs. Therefore, it can be concluded that sustained Cr(VI) reduction occurred via a closely coupled, biotic-abiotic reductive pathway in the flow-cell experiments.
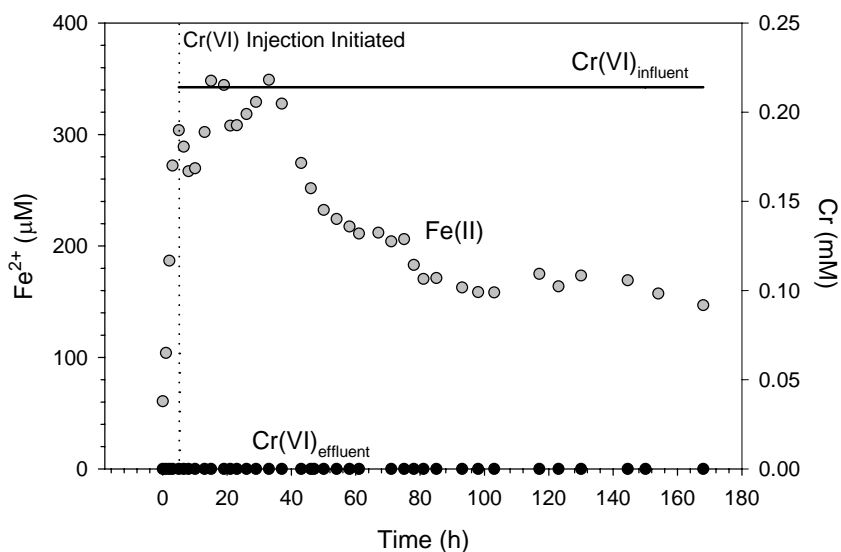

Figure 2. Comparison of temporal changes in influent and effluent aqueous Cr(VI) and Fe(II) concentrations for ferrihydrite reduction by *S. alga*.

The compositional evolution, speciation, and structural environment of Cr and Fe within the solid-phase products formed during Cr(VI) reduction was studied using extended x-ray absorption fine structure (EXAFS) spectroscopy conducted on Beam Lines 4-1 and 4-3 at the Stanford Synchrotron Radiation Laboratory. EXAFS measurements of the solid-phase products revealed that Cr(III) occurs in a mixed Fe(III)-Cr(III) hydroxide of the general formula $Fe_{1-x}Cr_x(OH)_3 \cdot nH_2O$, having an α/β-FeOOH local order (Hansel *et al.*, 2003). Fourier transforms (FTs) from Cr K-edge EXAFS spectra of the products at 70 h (relatively "young"

stage) and 168 h (should contain substantial amounts of recycled Fe(III)) reaction times are compared to a series of Fe(III)-Cr(III) hydroxide models in Figure 3. The radial structure at distances > 2 Å in the 70 h sample FT is significantly different than in the 168 h sample FT, indicating the presence of differences in the solid phase products.

Comparison of the spectra for the reaction products to the model spectra allows *in-situ* quantification of the Cr:Fe ratio within the solids (Hansel *et al.*, 2003). Solids formed after 70 h of reaction have an approximate Cr-to-Fe ratio of 1:2.5 ($Fe_{0.7}Cr_{0.3}(OH)_3 \cdot nH_2O$). This compares to a ratio of 1:3 that would be predicted for phases produced via the reaction: $3Fe^{2+} + HCrO_4^- + 8H_2O \rightarrow 4Cr_{0.25}Fe_{0.75}(OH)_3 + 5H^+$. In contrast, the 168 h reaction products have a Cr-to-Fe ratio of 2.5:1 ($Fe_{0.3}Cr_{0.7}(OH)_3 \cdot nH_2O$). The time-dependent increase in this ratio strongly suggests that microbial reduction of Fe(III) within the mixed Fe(III)-Cr(III) hydroxides occurred, whereby solids undergoing continued reaction were enriched in Cr(III) relative to those at 70 h. Thus, as the reaction proceeds, Fe within the system is cycled (*i.e.*, Fe(III) within the Cr, Fe hydroxide reaction product is further reduced by *S. alga* to Fe(II) and available for continued Cr reduction) and the hydroxide products become enriched in Cr relative to Fe.

The predicted solubility of the Cr(III) products is plotted in Figure 4. The solubility of $Fe_{1-x}Cr_x(OH)_3 \cdot nH_2O$ phases increases as the mole fraction of Cr(III) within the solid increases according to the equation $\log K_s = 4.23 - 0.172(1-x)^2 - 1.392(1-x)^3 + \log x$, where x is the Cr(III) mole fraction (Rai *et al.*, 1986). As such, conversion of Cr(III) in the solid-phase products from $Fe_{0.7}Cr_{0.3}(OH)_3 \cdot nH_2O$ (70 hr reaction) to $Fe_{0.3}Cr_{0.7}(OH)_3 \cdot nH_2O$ (168 hr) leads to an order-of-magnitude increase in Cr(III) solubility. Under conditions of sustained Cr(VI) reduction, purification of Cr(III) within the solid may lead to a pure Cr hydroxide phase, which is considerably more soluble than the observed Fe, Cr solid-solution phases. Nevertheless, the overall solubility of Cr is substantially diminished through the initial reduction of Cr(VI) to the less soluble Cr(III) hydroxides. In light of these findings, the ultimate solubility of Cr(III) in mature, bioremediated systems may be predicted from that of $Cr(OH)_{3(s)}$.
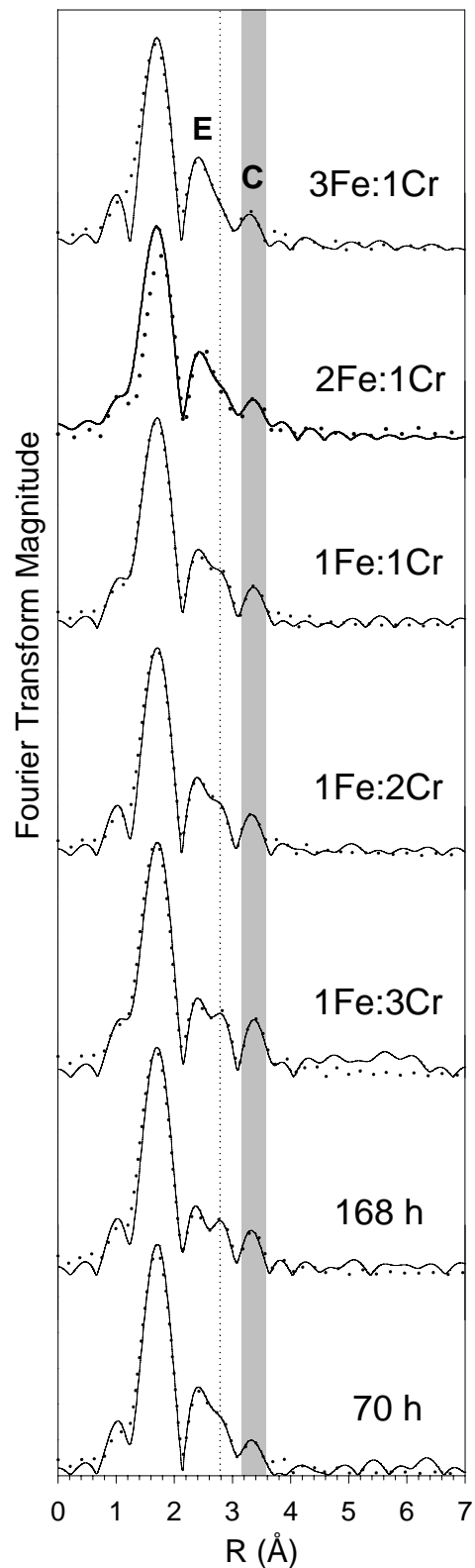

Figure 3. Fourier transforms for Cr standards (ratio of Fe to Cr in solid indicated) and solid-phase products for two time points following indirect Cr(VI) reduction by bacterially generated ferrous iron. All data (solid line) were fit (dotted line) over k=3 to 10.5 Å^{-1} for consistency among spectra. Edge- (E) and corner-sharing (C) contributions are indicated.
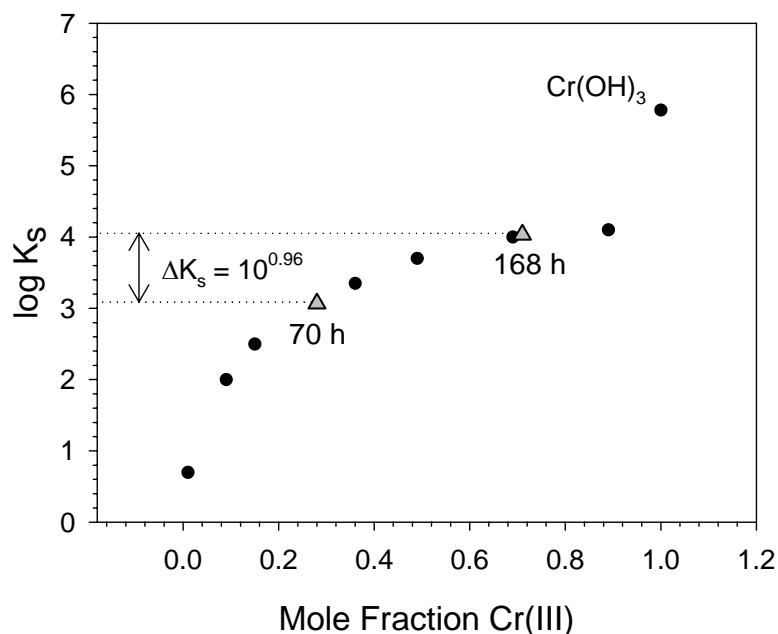
Figure 4. Solubility curve for $Fe_{1-x}Cr_x(OH)_3 \cdot nH_2O$ precipitates as a function of mole fraction of Cr(III) (circles) according to $\log K_s = 4.23 - 0.172(1-x)^2 - 1.392(1-x)^3 + \log x$ (Rai et al., 1986). Chromium(III) mole fractions for the solid-phases from two time points (triangles) determined from Fourier transform comparative analysis are included to estimate the relative solubility of the two solid-phase products.

References

1. Fendorf S., Wielinga B. W., and Hansel C. M. (2000) *Internat. Geol.* **42**, 691-701.
2. Hansel C.M., Wielinga B.W., Fendorf S. (2003) *Geochim. Cosmochim. Acta* **67**, 401-412.
3. James B. R. and Bartlett R. J. (1983) *J. Environ. Qual.* **12**, 169-172.
4. National Research Council (1974) Medical and biological effects of environmental pollutants: chromium. National Academy of Science.
5. Rai D., Zachara J., Eary L., Girvin D. C., Moore C. A., Resch C. T., Sass B. M., and Schmidt R.L. (1986) Geochemical Behavior of Chromium Species, final report. Electric Power Res. Inst.
6. Sass B. M. and Rai D. (1987) *Inorg. Chem.* **26**, 2228-2232.
7. Wielinga B., Mizuba M. M., Hansel C. M., and Fendorf S. (2001) *Environ. Sci. Technol.* **35**, 522-527.